optics

MDPI

Article

Higher-Dimensional Communications Using Multimode Fibers and Compact Components to Enable a Dense Set of Communicating Channels

Daniel A. Nolan

Science & Technology Division, Corning Research & Development Corporation, Corning, NY 14831, USA; danielnolan42@outlook.com

Abstract: Higher-dimensional communications are of interest for multiple reasons, including increasing the classical transmission capacity and, more recently, the quantum state transfer through fibers using the many modes within the fiber. For quantum communications, this enables an increase in the number of bits per photon, increasing quantum fidelity, increasing error thresholds and enabling hyperentanglement transfer, among other possibilities. A high-dimensional quantum state transfer can be transported through multimode fiber using the many modes available. However, this transfer of information through multimode optical fiber is limited by attenuation and mode coupling among the various spatial and polarization modes. Here, we consider how this mode coupling impacts the transfer process. We consider the fiber's modal properties, including orbital angular momentum, modal group numbers, and principal modes. We also investigate and propose input and output optical components, as well as fiber properties, which better mitigate the deleterious effects of mode coupling. We use the WKB approximation to the scaler wave equation as a guidance to quantify this coupling and then implement corrections to this approximation using exact solutions to the scaler wave equation. We consider methods to circumvent this mode coupling using optical fiber designs, holographic optical components and devices that are commercially available today. Some of these components, such as the holographic gratings and lenses, could be implemented using flat optics.

Keywords: multidimensional communications; mode coupling; quantum key distribution input/output optics

Citation: Nolan, D.A. Higher-Dimensional Communications Using Multimode Fibers and Compact Components to Enable a Dense Set of Communicating Channels. *Optics* **2024**, *5*, 330–341. https://doi.org/10.3390/opt5030024

Academic Editor: Yasufumi Enami

Received: 28 June 2024
Revised: 28 July 2024
Accepted: 2 August 2024
Published: 7 August 2024

1. Introduction

Quantum communication is an important component of quantum information science. Among other aspects, quantum communication involves quantum state transfer among multiple nodes, including quantum computers and simulators and, in general, multiple communication sites. Quantum communication also, in principle, enables absolute secure communication among the parties involved. A very active area of research within quantum communications is quantum cryptography. Quantum cryptography enables secure communications between two points, termed Alice and Bob. There already exists a considerable amount of commercial deployment of quantum key distribution systems, QKDs, in both fiber-based and free space applications. Currently, the QKD is the driving technology behind the development of quantum state transfer. Progress continues in the development of new quantum sources, detectors and low-loss optical fibers. In general, there are two approaches to QKDs, discrete and continuous variables. Discrete quantum communication linking distances more than hundreds of kilometers [1–3] has been achieved. New concepts such as twin-field QKDs [4] have enabled point-to-point links of over 800 km. Continuous-variable QKDs take advantage of the wave nature of light by using a homodyne detector [5]. Distances of over 200 km have been achieved [6], as well as demonstrations of over 15 km using seven-core multicore fiber [7].

Quantum key distribution using entangled photons is currently under intense research. Entangled photon states are non-separable and as such enable the possibility of implementing quantum nodes, utilizing quantum memories and repeaters for quantum information networks [8]. These systems take advantage of the fact that two photons are entangled in polarization, frequency or time. The quantum photon can be in one of two states, and this is encoded as a qubit. Beyond two-dimensional entanglement is higher-dimensional entanglement and hyperentanglement. Hyperentanglement [9], is simultaneous entanglement in multiple, rather than just two, degrees of freedom. Examples of the other degrees of freedom include polarization, space, time and frequency. The advantages of communicating with higher-order entanglement (using qudits rather than qubits) include increasing the quantum transfer capacity, increasing the number of bits per photon, increasing quantum fidelity and increasing the error threshold. The transfer of higher-dimensional states in optical fiber is of significant research interest. Demonstrations in both multimode [10] and in multicore [11] fiber have been reported. In multimode fiber, the distribution of high-dimensional orbital angular momentum over 1 km of few-mode fiber has been demonstrated, using an actively stabilizing phase pre-compensation technique to overcome the negative effects of spatial and polarization mode coupling [9]. Finally, it is important to mention some of the challenges of high-dimensional quantum communication that have recently been documented [12].

There are many important aspects to the transmission of higher-dimensional (modal) communications through optical fiber. This includes the active sources and devices required for the transmission and signal processing, as in silicon photonics processing [13], as well as systems considerations, such as the required amplifiers for longer transmission distances [14]. In this report, we limit ourselves to the implementation of input and output passive optical components, as well as fiber index profiles, to enable better simultaneous–higher-dimensional quantum communication over multiple channels. We consider fiber-optical properties, as well as the compatible input/output optics that best enable the entire quantum communication system to function. The passive optical components are those compatible with free space connectivity and those that are either commercially available or are currently undergoing intensive global research activity via metasurfaces. The available components and devices considered include spatial light modulators, gratings and lenses, among others. Longer term, it is expected that the implementation of these components will be enabled with flat optics, rather than bulk optical components. We use data from the literature to substantiate the viability of other components for higher-dimensional quantum communication systems. The idea of using holographic gratings to couple array sources and detectors to the specific LP11 optical fiber mode has been proposed and implemented [15]. This enables the simultaneously transmission of four channels. That is, two spatial modes times two polarization modes, $2 \times 2 = 4$ modes. Here, we investigate how to scale this idea to many modes and show that it is very possible to scale to 20 or more spatial–polarization modes.

We consider the modal properties of the transmitting optical fiber, including orbital angular momentum, mode groups and principal modes. The possibility of transmitting information free from the deleterious effects of mode coupling, the width of the transmission temporal window and the minimum optical loss are important to understanding the viability of high-dimension quantum communications.

In Section 2, we focus on the modal properties of the fiber and how the fiber's index profile affects the intermodal and intramodal temporal bandwidth, as well as how this profile affects the input and output optical component requirements. We discuss the relationship of the orbital angular momentum modes with intermodal and intramodal temporal delays. We investigate the use of a step index fiber profile to better enable one to target specific modal groups and modes within a modal group. We model the phase grating properties that map the spatial distribution of the laser and detection array distribution with the specific inter and intra modes of the fiber.

In Section 3, we point out the limitations to the WKB approximation. Exact solutions to the wave equation show that a break in the degeneracies of the modes within a modal

group occurs. Also, there is a distribution of the input/output angles of the modes, rather than a single value, and this affects the achievable coupling efficiencies and modal cross-talk at the input/output.

In Section 4, we discuss the principal modes and show how they can be used to deal with mode coupling and to enable node-to-node quantum communication, using the many intra modes of the fiber. These principal modes are only used with the intra modes because the fiber design prevents inter modal coupling.

In Section 5, Outlook, we discuss the current situation, including the consequences of implementing the corrections to the WKB approximation. We also discuss the availability of the disclosed devices and components, as well as the possibility of substituting flat optics components and devices for the bulk components described.

2. High-Dimensional Quantum State Propagation in Fiber and the Associated Input and Output Components

The intent here is to consider higher-dimensional quantum communication, including the fiber and input and output components, as an entity. We propose the optimization of the optics, as opposed to optimizing the fiber and then separately optimizing the input/output optics. In this way, we enable a denser communication system, a system that enables parallel processing in separate modal channels in the presence of mode coupling. We propose a system where the processing of quantum signals propagates within the modal groups of the fiber, as opposed as to specific modes such as OAM modes.

Mode coupling among the modes within a modal group occurs almost spontaneously, since these modes are degenerate amongst themselves. This is according to the WKB approximation, which has to be exact for an infinitely parabolic index profile. Although, there are differences between the exact solution and the WKB approximation, as the effective index of the mode groups approaches that of the cladding index. In this case, there is a splitting of the modal groups. For degenerate modes, only the slightest perturbation in a deployed fiber, such as twisting or bending, will cause the mixing of information among the communicating spatial channels. Mode coupling in multimode fiber has been documented well within the literature; see, for example, reference [16]. In an alpha index fiber profile [17] the modal groups, mode numbers and modes within a modal group are determined by the core–clad index difference, the radius of the core and the propagating wavelength. In an alpha index profile, one can keep the same number of modal groups, and at the same time minimize the amount of mode coupling from modal group to modal group, by increasing the core delta and decreasing the core radius. This is true, regardless of the alpha parameter of the profile, the step index (alpha of infinity) vs alpha of parabolic (alpha = 2), for example. This approach enables the isolation of quantum channels using the modal groups. Mode coupling will occur within a cabled and deployed optical fiber when the propagation distances are significant within a degenerate modal group. This includes the OAM modes, because typically OAM modes are degenerate with other OAM modes within a modal group. This is especially true of OAM modes of an equal radial number and opposite azimuthal number, again because they are degenerate. This has been evidenced in a specially designed ring-core fiber [18]. Here there is a temporal broadening of the pulses propagating in OAM modes of an opposite azimuthal number, which the authors say is similar to polarization mode dispersion due to polarization mode coupling.

MIMO (modes in–modes out) [19] is a classical optical communication technology that enables one to deal with this issue. However, MIMO requires significant power, and for this reason, it cannot be used with quantum systems. An alternative approach, principal mode communication, is possible but is less developed and involves a number of special optical components, including active components, some of which are not yet commercialized. We discuss this approach for quantum communications in Section 3. Modal pre-compensation [10] is a relatively new approach to deal with mode coupling and is just now being considered for quantum communications.

Inputting signals into a fiber and targeting modal groups is difficult, especially when launching into modal groups beyond M = 1. However, it has been proposed that this is less difficult when the transmission fiber is a step index fiber [20]. Although the modal groups in a step index fiber separate significantly in time as they propagate, the coupling from modal group to modal group can be insignificant for a larger index delta and smaller core radius. A step index fiber for space division multiplexing was first proposed by Cedarquest [20] as early as 1984. He proposed using a step index fiber, because to a first approximation, the WKB approximation, the mode power distribution only depends on a specific angle and therefore simplifies the input. However, the angle of propagation is not singular, but there exists a distribution in angle around a centroid value. Again, the WKB approximation is only a guide and good starting point.

2.1. Intermodal Coupling

Cederquist [20] proposed methods to couple light into and out of the modal groups of a step index fiber using a computer-generated hologram. One of his methods enabled him to input a point source of light to a desired modal group. In another method, he showed how to input a strip of light into targeted modal groups. However, it was not shown how to input separate modes within a modal group. Later, Huang [21], based on the previous work of Berkout [22] and Lavery [15], used a lens to input light to the modes within the second modal group of a parabolic fiber, but this method is not scalable to more modal groups. Huang did, however, demonstrate MIMO using this second modal group. In another implementation of higher-order modes, Mirhosseini [23] demonstrated quantum cryptography using both OAM and angular modes.

Here, we describe a new optical method to couple to and from modal groups in a step index fiber, based on the WKB approximation. Higher-order correction will be considered in Section 3.

Below is a diagram showing light exiting a multimode group. For a step index fiber, all the modes exit the fiber at a specific angle characteristic of that group.

In a step index profile, each modal group exits the fiber around an angular centroid, an annular cone. Lenses and holograms or metasurfaces can impose a geometric transformation—outputting the modal groups onto a linear array detector. The higher the output angle of the modal group, the further the light is removed in the X direction. In addition, the length of the array is longer in the Y direction. This is made possible by putting a phase plate (e.g., metasurface, SLM or etched array) after the lens in Figure 1.

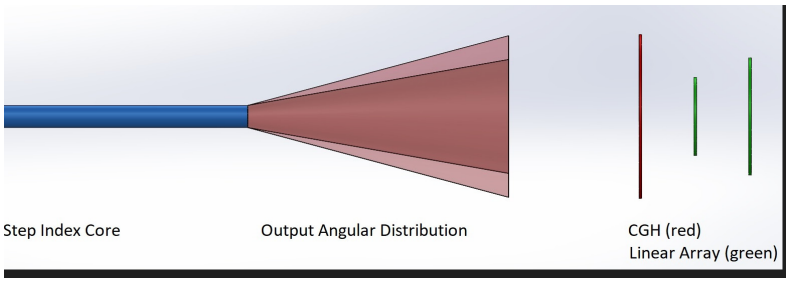

Figure 1. Z > propagation direction.

Below, we show pictorially how different modal groups' angular cones are transformed to linear optical arrays after the light traverses the phase plate (Figure 2).

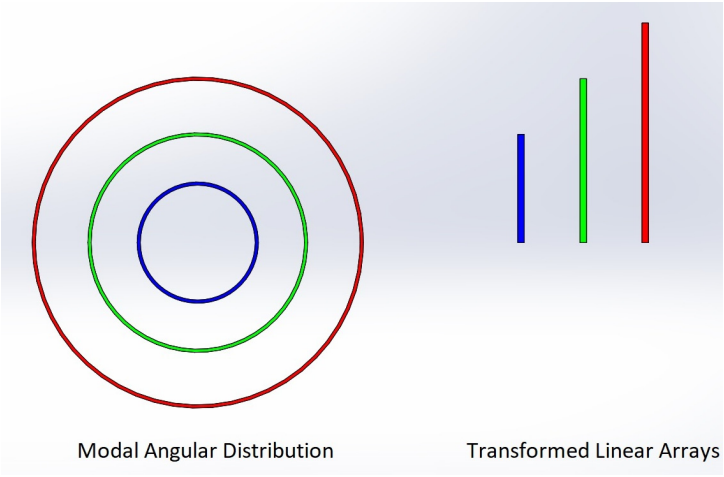

Figure 2. How different modal groups' angular cones are transformed to linear optical arrays after the light traverses the phase plate.

Now, we determine the phase plate values for the azimuthal angles of the angular cone. We use the optical phase transformations disclosed in reference [22] by Berkhout, which are an improvement over those of Cederquist [20]. In this equation, the values of a and b are arbitrary, with dimensions of length.

$$\phi(x,y) = -\frac{2\pi a}{\lambda f}\left[y\tan^{-1}\left(\frac{y}{x}\right) - x\ln\left(\frac{\sqrt{x^2+y^2}}{b}\right) + x\right] \quad (1)$$

Here, x, y are positions around the annular ring of the modal group light cone; a is a free parameter that dictates the length of the focused strip and how far the strip shifts along the x axis; f is the focal length of the Fourier lens; λ the wavelength; and b acts as a scaling factor.

Here, we show an example phase plate used to convert the light of an angular cone to light of a rectangular distribution. The light from the fiber is assumed to be that of a cone exiting at a specific angle and then intercepting the plate with a radius of 250 microns. The calculated phase differences, in microns, around the ring (0 to 2 pi) are shown below These micron delays can be converted to fractions of wavelength for the use of an SLM, or spatial light modulator (Figure 3).

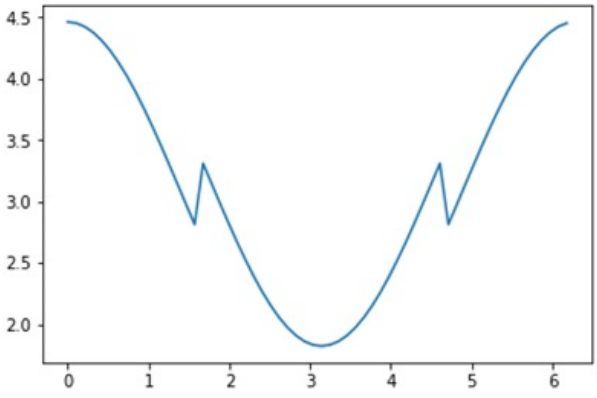

Figure 3. Calculated phase delay differences, phi (phase plate value) vs. theta (angle around an azimuthal ring of the plate at a specific radius). X axis, azimuthal angle [radians]; Y axis, phase delay values, $\varphi(\theta)$.

In order to generate this phase delay around each modal ring position, one can use a metasurface plate or even a spatial light modulator. One can implement polarization-dependent versions or polarization-independent versions. Metasurface designs can be implemented using an RCWA (rigorous coupled wave analysis) algorithm. SLMs are polarization-dependent but can be configured to be polarization-independent [24].

In reference [20], Cedarquist et. al. showed an optical component arrangement to transform an input ring of light into a linear strip of light, which could then be focused onto a detector. The ring of light results from the collimation of angular modal group cones, output from a step index fiber. The phase delay component can be fabricated with a metasurface or computer-generated hologram and is placed between lenses, as in Figure 4 below.

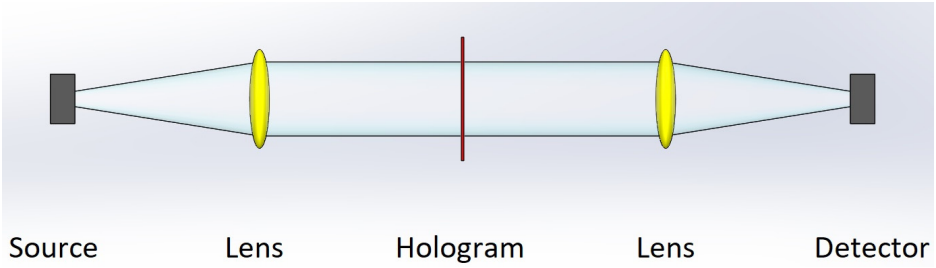

Figure 4. Optical configuration to implement the phase hologram.

According to ref [13], for a step index fiber, the number, M, of modal groups is

$$M = n1 \times ka \times \sqrt{\Delta/2} \tag{2}$$

where $n1$ is the index of the core, $k = 2\pi/\lambda$, λ is the wavelength and $\Delta = (n1 - n2)/n1$, where $n2$ is the index of the cladding.

The angular offset to input light into a particular modal group, m, is

$$\sin(\theta_m) = n1 \times \sqrt{2\Delta} \times m/M \tag{3}$$

So that

$$\theta_m = \arcsin\left(n1 \times \sqrt{2\Delta} \times (m/M)\right) \tag{4}$$

For a step index fiber, the angular input/output values increase linearly with the modal group number. As an example, for Δ = 0.01, and a = 9 microns, M = 3.7 and the angular input/output values (Table 1) are as follows:

Table 1. The angular input/output values.

m	θ_m
1	3.14
2	6.29
3	9.46

For MIMO (modes in–modes out) applications, each angular output cone is transformed to a linear strip as described above. There at the linear strip, a detector array can be placed. The number of detectors will be equal to the number of modes within that modal group. To minimize the digital processing temporal window, it is desirable to enable strong mode coupling throughout the transport path. So, intramode coupling at the input and output sites is not of concern but encouraged. It does matter, though, that light is efficiently coupled into and out of a specific modal group.

2.2. Coupling from a Linear Array to Spatial Modes within a Modal Group

The coordinate transformations of modal groups exiting the fiber are transformed by a phase grating implemented with an SLM, metasurface or etched glass. A given modal group transforms to positions on a linear strip (e.g., detector array)

The modal group's light exit cone can be further characterized with an azimuthal angle. Specific azimuthal angles transform to positions on the linear strip (Figure 5). The azimuthal zero angle begins on the positive x axis.

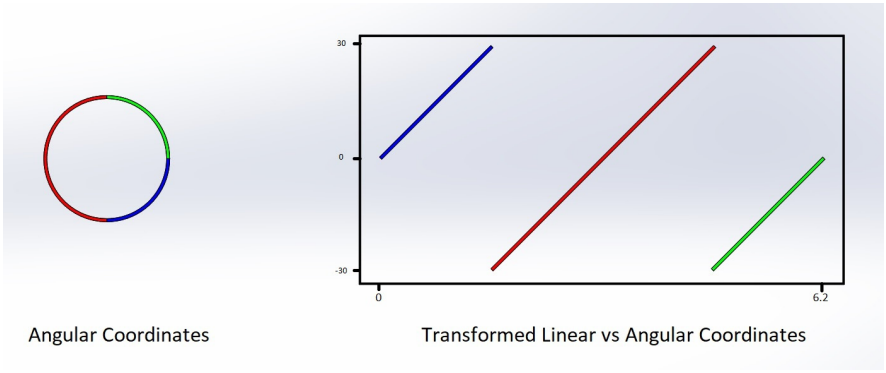

Figure 5. Angular distribution of 3 superimposed intra modes.

Light along the exit cone–angular position transforms to a position on the strip. The spatial transmission is double-valued, in that two positions on the arc correspond to one position on the linear strip. This indicates that there is modal coupling, as the modes within a modal group undergo a coordinate transformation.

There are m spatial groups within the mth mode and two polarizations for each spatial mode. As for multiplexing within a modal group, it is not necessary to multiplex with a specific modal group. In fact, it is proposed here to multiplex with subgroups within the modal group. The modal group can be separated into m subgroups; each subgroup is composed of a different combination of spatial modes.

$$X_j = \sum_{j=1}^{m} C_{ji} X_i \tag{5}$$

The transformed angular cone is transformed to a linear strip, and the linear strip is sectioned into m sections. The subsections are physical regions of overlap with a specific source or detector in an array. The figure below is an example of an arc with four sections and four subgroups, because the transformation is double-valued. A linear array of sources, for example, transforms to the group mode cone, such that a source in the array couples to two arcs on the angular cone spaced 180 degrees apart. For example, if we have four sources, color coded (blue, green, red, orange) on a linear strip, they will transform to two opposite positions on the arc. This is shown in Figure 6 below.

In addition to mode-coupling concerns, it is important that attenuation is addressed. For quantum key distributions [1–4], attenuation is of major concern. The transportation of a single photon is detected with a quantum detector, but the probability of detecting such a photon is in the order of -20 dB down and even less. In these references, it is shown how this low probability can be dealt with. The higher modal groups for quantum transportation will always be of higher attenuation than the fundamental mode. This is due to micro and macro bending. The attenuation of light in the fundamental mode is in the order of 0.15 dB/km. The attenuation of the higher modes will always be more, and it is expected that this value will increase with the mode number. This will be the subject of further research, including applications for higher-order quantum key distribution and also quantum routing.

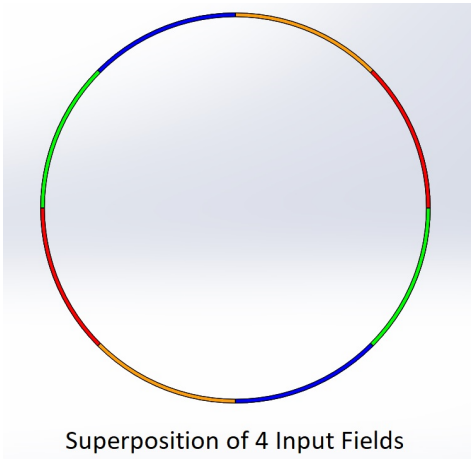

Figure 6. This shows how four sources geometrically arranged as a linear array (blue, green, red and orange) transform to the azimuthal positions on the angular cone of a step index fiber, all within a modal group.

3. Corrections to the WKB Approximation

The WKB approximation has been used extensively to solve the propagation and modal properties of an optical fiber [17]. This method is often used as a guidance to set the fiber parameters and then implement more exact calculations. In this approximation, the field can be forced to be zero at the core cladding boundary. This method gives the exact solutions for the modal eigenvalues for a parabolic index profile, but the presence of cladding distorts these values. So, it is important to consider that corrections to this approximation for our case here, and for this reason, we look at the scaler wave equation for an optical fiber and we assume that the fiber is of circular symmetry.

The wave equation for the modes within an optical fiber is

$$\bigtriangledown^2 E + k0^2 n^2(r) E = 0 \tag{6}$$

where $n(r)$ is the index profile of the fiber and ko is 2 π/λ, and λ is the wavelength of light.

The wave equation describes well the propagation properties of the modes within a circular multimode fiber for low index differences between the core and cladding index values, typical for telecommunication fibers. The WKB approximation to the wave equation enables us to determine the first-order properties of the propagation, but it is important to consider its limitations. The wave equation, Equation (6), can be solved exactly using an eigenvalue expansion method; see, for example, Meunier [25]. Here, we model the modal propagation output from a fiber and the subsequent propagation through the system of Figure 4. We use the step index fiber properties of [18], a core cladding index difference, Δ, of 1% and a core radius of 9 microns. This gives us 4 modal groups and 10 spatial modes, each with two polarizations, for a total of 20 modal channels

The solution to the wave equation gives the modal eigenvalues, propagation constants, and eigenfunctions and fields. These modes can be quantified with a radial number (μ) and an azimuthal number (ν). Typically, one can solve a series of radial modes, μ, for a specific azimuthal mode, for example, ν = 0 or ν = 1, etc. Using this method, we obtained the same propagation constants as those shown for a step index profile in ref [24]. The eigenfunctions for these modes can be used to obtain the field distributions for the modes discussed in Section 2. We can also solve for the angular distribution of light output from the fiber using the far-field methods shown in [26]. The first important result is that the angular output cannot be quantified using a single specific angle, but rather an angular distribution of light results, even for a step index fiber. We found that the modal angular output distributions result in cross-talk between the modal groups, and this cross-talk is on the order of -10 dB for the first four modal groups of a step index fiber, excluding (attenuating) the LP12 (μ = 1,

ν = 1) mode to maintain this low level of modal group cross-talk. Angular filters can be used to further minimize this unwanted cross-talk.

As an example, the output distribution of LP21 is (ν = 2, μ = 0), on a screen 1 cm from the fiber.

The second important result in using the solutions to the scaler wave equation is that this output angular distribution (not a specific angle) causes interference effects exiting the circular to rectangular hologram of Figure 4. Similar interference patterns are shown in [22]. Berkhout [22] proposes a second hologram based on the principal of a stationary phase in order to deal with this complicated interference. The second hologram can be placed on the opposite side of a glass on which the first hologram is deposited. The importance of this second hologram is also discussed in Refs. [27,28]. This holographic grating is described using the equation

$$\phi(x,y) = -2\pi ab/(\lambda f)\exp\left(-\frac{x}{a}\right)\cos\left(\frac{y}{a}\right) \quad (7)$$

Here, a and b are parameters to enable a scaling of the free space propagation following the hologram.

Now, we model the modal propagation output from a fiber and the subsequent propagation through the system of Figure 4. We use the step index fiber properties of [18], a core cladding index difference, Δ, of 1% and a core radius of 9 microns. This gives us 4 modal groups and 10 spatial modes; each spatial mode includes two polarizations, for a total of 20 modal channels. We use the hologram described by Equation (1) above and also consider adding the second hologram of Equation (7), The holograms are inserted between the two lenses of Figure 4. The first hologram converts the geometry of the light form from circular to rectangular, and the second hologram corrects the complex interference effects patterns. We use Python LightPipes 2.1.5 to model the entire free space propagation. In LightPipes, we use a grid size of 200 × 200 and a pixel size of 10 microns. The grid is centered to capture the field, of which the power is shown in Figure 7. The center of the grid is at position x = 100, y = 100. The output of the calculation for three mode groups, along the x axis (y = 100), is shown in Figure 8. The light does focus onto sequential grid positions 110, 130, 140. But there exist spurious peaks, which are due to the limitations of the model–grid size, but also due to interference patterns exiting the holograms. This Python LightPipes model will require further investigation, as the spurious noise is in part real and in part due to the limitations of the grid calculations. But with the second hologram, the light output does focus onto a rectangular grid, offset from the center and to the right quadrant. So, here we have a very interesting fiber–free space platform for space division multiplexing analysis.

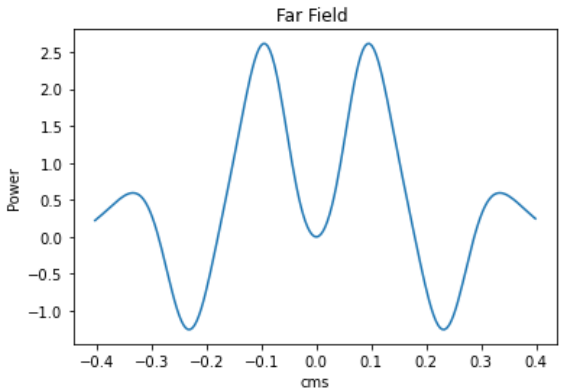

Figure 7. Shows the output power calculated from the LP21 mode at a screen 1 cm from the fiber.

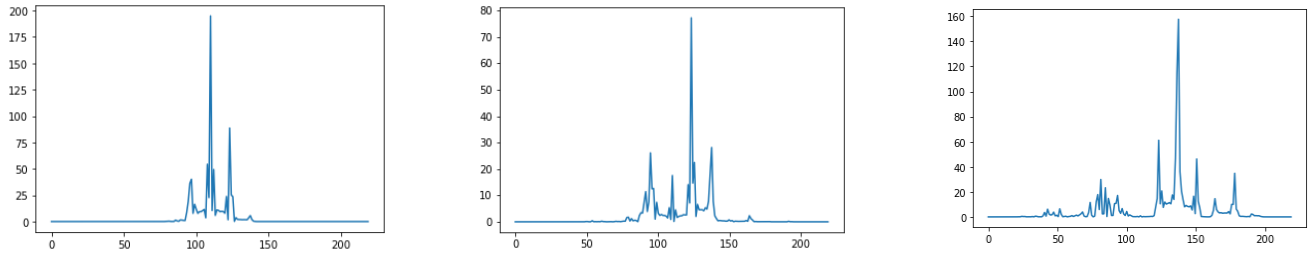

Figure 8. Python LightPipes simulation—output in a. u. for the optical component system shown in Figure 4, with radial mode number μ = 0 and azimuthal mode number ν = 0, 1, 2, and within group numbers M = 1, 2, 3 sequentially.

4. Principal Mode Propagation

Principal mode propagation in an optical fiber is a method to deal with the intramode coupling that occurs among the propagating modes of the fiber. Such a mode coupling can be significant enough that the output mode signal is completely scrambled. Vectorial–modal pre-compensation [9] is another method to deal with mode coupling. Although this is an important approach and, we can expect, useful for this application, we will not consider this further in this report and only focus on principal mode propagation. Using principal modes, which are a superposition of guided modes, one can transmit an optical signal through a fiber in the presence of significant mode coupling and then output the pulse to a principal mode, all being accomplished with the output signal being free from pulse distortion.

The principal modes in a highly multimode fiber have been characterized using interferometric methods and temporal based methods. Using fibers of meter lengths [29–32]. The temporal-based method [31,33] has been used to determine a few principal modes over kilometer lengths. These methods assume no or little optical loss during the propagation and launch and detection. Methods to deal with launch conditions and also optical loss have been discussed in the literature [34,35]. In this discussion, we assume no excess loss, including the input/output optics, as well as pulse propagation within the propagating fiber.

An important parameter is the temporal window of the arrival times that a photon can take as it propagates through the fiber and among the possible guided modes. This temporal window must be wide enough to include all the possible modal path arrival times. The window of arrival times for subsequent signal pulses must not overlap with the windows of previous pulses.

So, we propose to use principal mode transmission only among the modes within a modal group, i.e., the intra modes. We can consider the guided modes of Figure 6. Each of these modes is a superposition of eigenmodes of the step index fiber. Remember, in a step index fiber, each modal group propagates as an angular cone but broadened in angle, and the modes within a modal group can be characterized as a superposition of the guided modes within that modal group. We can determine the principal modes from the spatial sectors of Figure 6. These principal modes can be determined using either the interferometric method or the time delay method. The principal modes change in time. This time is estimated to be on the order of seconds, and because of this, the principal modes will need constant adjustment. This can be done first using classical, higher-powered light, and once determined, single photons can be launched accordingly, as specified. Launching and detecting the principal modes will require an optical component configuration of Figure 4. This will require the use of lenses and a tunable device such as a spatial light modulator. It is expected that the lenses can be replaced with flat optics components, currently undergoing global research.

5. Outlook/Conclusions

Currently, higher-dimensional quantum communication is undergoing global research for the reasons discussed above. Here, we have proposed a method to implement simultaneously many channels of communication through fibers. We used the WKB approximation as a guidance to deal with the mode coupling that occurs when inputting and outputting light to the fiber, as well as the mode coupling that occurs within the fiber during transmission. We then used the exact solutions to the scaler equation to quantify the corrections to the WKB approximation regarding the input/output coupling. These corrections are significant and show that cross-talk will occur at the input/output sites, but that this can be minimized using spatial filters. We also implemented a Python LightPipes algorithm to better understand and quantify how the light converts from a circular to a rectangular geometry and therefore how circular optical modes convert to the rectangular arrays of sources and detectors. To implement and commercialize these optical fiber-based quantum systems, there is a need to develop new optical components including tunable–deployable devices such a spatial light modulators, SLMs, as well as new compact optical components such as flat optics—lenses, phase plates, angular filters and gratings. Also, we can consider modems, described in [36] to the better separate the inter-modes. All, these devices will need to be suitable for telecom system deployment. Also, an attenuation target for the modal-dependent input/output optical components will be less than 1 dB per component. Meanwhile, the methods described here will need further research, to better determine the number of higher dimensions possible using the optical component configurations disclosed, as well as the optical fiber parameters, including mode-dependent coupling and mode-dependent attenuation.

Funding: This research received no external funding.

Institutional Review Board Statement: Not applicable.

Informed Consent Statement: Not applicable.

Data Availability Statement: Data is contained within the article.

Conflicts of Interest: Author Daniel A. Nolan was employed by the company Corning Inc.

References

1. Korzh, B.; Lim, C.C.W.; Houlmann, R.; Gisin, N.; Li, M.J.; Nolan, D.; Sanguinetti, B.; Thew, R.; Zbinden, H. Provably secure and practical quantum key distribution over 307 km of optical fibre. *Nat. Photonics* **2015**, *9*, 163–168. [CrossRef]
2. Yin, H.-L.; Chen, T.-Y.; Yu, Z.-W.; Liu, H.; You, L.-X.; Zhou, Y.-H.; Chen, S.-J.; Mao, Y.; Huang, M.-Q.; Zhang, W.-J.; et al. Measurement-Device-Independent Quantum Key Distribution over a 404 km Optical Fiber. *Phys. Rev. Lett.* **2016**, *117*, 190501. [CrossRef]
3. Boaron, A.; Boso, G.; Rusca, D.; Vulliez, C.; Autebert, C.; Caloz, M.; Zbinden, H. Secure Quantum Key Distribution over 421 km of Optical Fiber. *Phys. Rev. Lett.* **2018**, *121*, 190502. [CrossRef] [PubMed]
4. Lucamarini, M.; Yuan, Z.L.; Dynes, J.F.; Shields, A.J. Overcoming the rate—Distance limit of quantum key distribution without repeaters. *Nature* **2018**, *557*, 400–403. [CrossRef]
5. Braunstein, S.; Van Loock, P. Quantum information with continuous variables. *Rev. Mod. Phys.* **2005**, *77*, 513. [CrossRef]
6. Zhang, Y.; Chen, Z.; Pirandola, S.; Wang, X.; Zhou, C.; Chu, B.; Zhao, Y.; Xu, B.; Yu, S.; Guo, H. Long Distance Continuous Variable Quantum Key Distribution over 202.81 Km of Fiber. *Phys. Rev. Lett.* **2020**, *125*, 010502. [CrossRef] [PubMed]
7. Sarmiento, S.; Etcheverry, S.; Aldama, J.; Lopez, I.H.; Vidarte, L.T.; Xavier, G.B.; Nolan, D.A.; Stone, J.S.; Li, M.J.; Loeber, D.; et al. Continuous-variable quantum key distribution over a 15 km multicore fiber. *New J. Phys.* **2022**, *24*, 063011. [CrossRef]
8. Sangouard, N.; Simon, C.; De Riedmatten, H.; Gisin, N. Quantum repeaters, based on atomic ensembles and linear optics. *Rev. Mod. Phys.* **2011**, *83*, 33. [CrossRef]
9. Deng, F.-G.; Ren, B.-C.; Li, X.-H. Quantum hyperentanglement and its applications in quantum information processing. *Sci. Bull.* **2017**, *62*, 46–68. [CrossRef] [PubMed]
10. Cao, H.; Gao, S.-C.; Zhang, C.; Wang, J.; He, D.-Y.; Liu, B.-H.; Zhou, Z.-W.; Chen, Y.-J.; Li, Z.-H.; Yu, S.-Y.; et al. Distribution of high-dimensional orbital angular momentum entanglement over a 1 km few-mode fiber. *Optica* **2020**, *7*, 232–237. [CrossRef]
11. Ding, Y.; Bacco, D.; Dalgaard, K.; Cai, X.; Zhou, X.; Rottwitt, K.; Oxenløwe, L.K. High-dimensional quantum key distribution based on multicore fiber using silicon photonic integrated circuits. *npj Quantum Inf.* **2017**, *3*, 25. [CrossRef]
12. Cozzolino, D.; Da Lio, B.; Bacco, D.; Oxenløwe, L.K. High-Dimensional Quantum Communications: Benefis, Progress, and future Challenges. *Adv. Quantum Technol.* **2019**, *2*, 1900038. [CrossRef]

13. Mojaver, K.R.; Safaee, S.M.R.; Morrison, S.S.; Liboiron-Ladouceur, O. Recent Advancements in Mode Division Multiplexing for Communication and Computation in Silicon Photonics. *arXiv* **2024**, arXiv:2404.03582. [CrossRef]
14. Su, Y.; He, Y.; Chen, H.; Li, X.; Li, G. Perspective on Mode—Division Multiplexing. *Appl. Phys.* **2021**, *118*, 200502. [CrossRef]
15. Lavery, M.P.J.; Robertson, D.J.; Berkhout, G.C.G.; Love, G.D.; Padgett, M.J.; Courtial, J. Refractive elements for the measurement of the orbital angular momentum of a single photon. *Opt. Express* **2012**, *20*, 2110–2115. [CrossRef]
16. Ho, K.-P.; Kahn, J.M. Mode coupling and its impact on spatially multiplexed systems. In *Optical Fiber Communications*; Kaminow, I., Li, T., Willner, A., Eds.; Academic Press: Cambridge, MA, USA, 2013.
17. Keck, D.B. Optical Fiber Waveguides. In *Fundamental of Optical Fiber Waveguides*; Barnoski, M., Ed.; Academic Press: New York, NY, USA, 1981.
18. Ge, D.; Gao, Y.; Yang, Y.; Shen, L.; Li, Z.; Chen, Z.; Li, J. A 6-LP mode ultralow-modal-crosstalk double ring-core FMF for weakly-coupled MDM transmission. *Opt. Commun.* **2019**, *451*, 97–103. [CrossRef]
19. Karadimitrakis, A.; Debbah, M.; Moustakas, A.L. Optical MIMO: Results and analysis. In Proceedings of the 2014 11th International Symposium on Wireless Communications Systems, Barcelona, Spain, 26–29 August 2014. [CrossRef]
20. Cederquist, J.N.; Tai, A.M. Computer-generated holograms for geometric transformations. *Appl. Opt.* **1984**, *23*, 3099–3104. [CrossRef] [PubMed]
21. Huang, H.; Milione, G.; Lavery, M.P.; Xie, G.; Ren, Y.; Cao, Y.; Willner, A.E. Mode division multiplexing using an orbital angular momentum sorter and MIMO=DSP over a graded-index few mode optical fibre. *Sci. Rep.* **2015**, *5*, 14931. [CrossRef] [PubMed]
22. Berkhout, G.C.G.; Lavery, M.P.J.; Courtial, J.; Beijersbergen, M.W.; Padgett, M.J. Efficient Sorting of Orbital Momentum States of Light. *Phys. Rev. Lett.* **2010**, *105*, 153601. [CrossRef]
23. Mirhosseini, M.; Magaña-Loaiza, O.S.; O'Sullivan, M.N.; Rodenburg, B.; Malik, M.; Lavery, M.P.; Boyd, R.W. High-dimensional quantum cryptography with twisted light. *New J. Phys.* **2015**, *17*, 033033. [CrossRef]
24. Liu, J.; Wang, J. Demonstration of Polarization-insensitive a spatial light modulation using a single polarization-sensitive spatial light modulator Modulator. *Sci. Rep.* **2015**, *6*, 9959. [CrossRef] [PubMed]
25. Meunier, J.P.; Pigeon, J.; Massot, J.N. A general approach to the numerical determination of modal propagation constants of optical fibers. *Opt. Quantum Electron.* **1981**, *13*, 71–83. [CrossRef]
26. Hayashi, T.; Tamura, Y.; Nagashima, T.; Yonezawa, K.; Taru, T.; Igarashi, K.; Tsuritani, T. Effective Area measurement of few—mode fiber using far field scan technique with Hankel transform generalized for chirality—asymmetric mode. *Opt. Express* **2018**, *26*, 11137. [CrossRef] [PubMed]
27. Stuff, M.; Cedarquist, J. Coordinate transformation realizable with multiple holographic optical elements. *J. Opt. Soc. Am. A* **1990**, *7*, 977–981. [CrossRef]
28. Hossack, J.; Darling, A.; Dahdouh, A.; Coordinate, J. Transformation with Multiple—Generated Optical Elements. *J. Mod. Opt.* **2007**, *34*, 1235–1250. [CrossRef]
29. Fan, S.; Kahn, J.M. Principal modes in multimode waveguides. *Opt. Lett.* **2005**, *30*, 135–137. [CrossRef] [PubMed]
30. Carpenter, J.; Eggleton, B.J.; Schröder, J. 110 × 110 Optical Mode Transfer Matrix Inversion. *Opt. Express* **2014**, *22*, 96–101. [CrossRef] [PubMed]
31. Milione, G.; Nolan, D.A.; Alfano, R.R. Determining Principal Modes in a Multimode Optical Fiber. *J. Opt. Soc. Am.* **2015**, *32*, 143–149. [CrossRef]
32. Xiong, W.; Ambichl, P.; Bromberg, Y.; Redding, B.; Rotter, S.; Cao, H. Principal Modes in Optical Fibers: Exploring the Crossover from Weak to Strong Mode Coupling. *Opt. Express* **2017**, *25*, 2709–2724. [CrossRef]
33. Nolan, D.A.; Nguyen, D.T. Light Localization and Principal Mode Propagation in Optical Fibers. *Front. Phys.* **2021**, *9*, 713085. [CrossRef]
34. Roudas, I.; Kwapisz, J.; Nolan, D.A. Optimal Launch States for the Measurement of Principal Modes in Optical Fibers. *J. Light. Technol.* **2018**, *36*, 4915–4931. [CrossRef]
35. Yang, J.; Nolan, D. Using Tomography for Characterizing Input Principal Modes in Optically Scattering Medium. *Opt. Express* **2016**, *24*, 27691–27701. [CrossRef] [PubMed]
36. Soifer, V.; Golub, M. *Laser Beam Mode Selection by Computer Generated Holograms*; CRC Press: Boca Raton, FL, USA, 1994.